

RESEARCH

Open Access



Apoptotic cell-derived extracellular vesicles-MTA1 confer radioresistance in cervical cancer by inducing cellular dormancy

Yuan-Run Deng^{1†}, Qiao-Zhi Wu^{1†}, Wan Zhang^{2,3}, Hui-Ping Jiang¹, Cai-Qiu Xu¹, Shao-Cheng Chen¹, Jing Fan¹, Sui-Qun Guo^{1*} and Xiao-Jing Chen^{4*}

Abstract

Background Radioresistance presents a major challenge in the treatment of cervical cancer (CC). Apoptotic tumor cells can create an “onco-regenerative niche,” contributing to radioresistance. However, the intercellular signaling mechanisms mediating the transfer of radioresistance from apoptotic to surviving cancer cells remain unclear.

Methods The role of apoptotic tumor cell-derived extracellular vesicles (apoEVs) in mediating radioresistance was investigated through integrated bioinformatics and experimental approaches. The GSE236738 dataset was analyzed to identify potential regulators, with subsequent validation of apoEV-MTA1 function using in vitro and in vivo models. Mechanistic studies focused on caspase-3 activation, p-STAT1 signaling pathway, and dormancy-associated protein networks. Furthermore, therapeutic strategies targeting MTA1 and its downstream signaling were evaluated for radiosensitization potential.

Results MTA1 was identified as a critical factor enriched in and transferred by apoEVs from apoptotic tumor cells to neighboring CC cells. Caspase-3 activation facilitated the nuclear export and encapsulation of MTA1 in apoEVs. Transferred MTA1 retained transcriptional activity, activated the p-STAT1 signaling pathway, and induced cellular dormancy via NR2F1, a key dormancy regulator, resulting in increased radioresistance. Knockdown of MTA1 in apoEVs or inhibition of p-STAT1 in recipient cells enhanced radiosensitivity. Furthermore, apoEV-MTA1 promoted tumor radioresistance and reduced survival rates in irradiated cervical cancer mouse model.

Conclusions This study demonstrates that apoEV-MTA1 confers radioresistance in CC by promoting cellular dormancy via the p-STAT1/NR2F1 signaling axis. Targeting this pathway could improve radiosensitivity and provide a promising therapeutic strategy for CC patients.

[†]Yuan-Run Deng and Qiao-Zhi Wu contributed equally to this work.

*Correspondence:

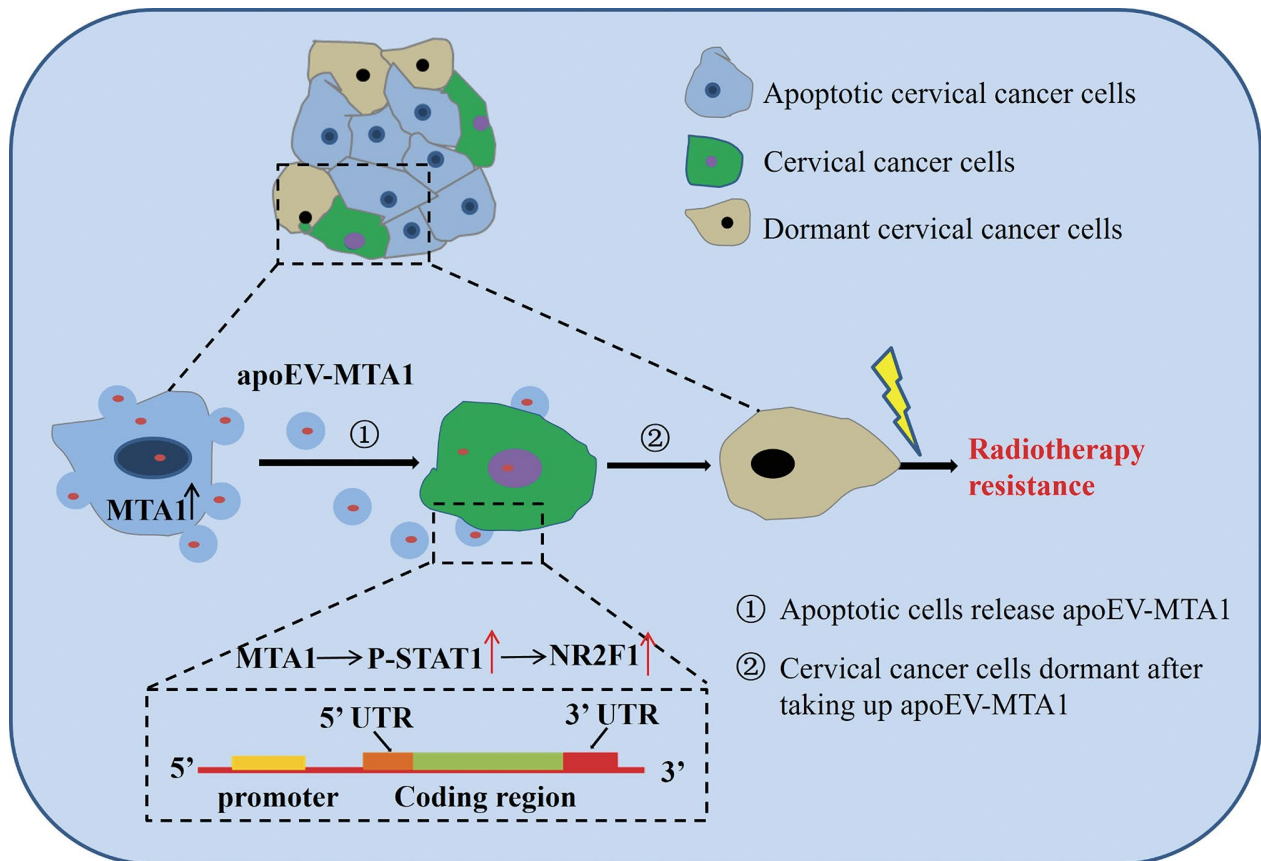
Sui-Qun Guo
guosq2005@126.com
Xiao-Jing Chen
291594799@qq.com

Full list of author information is available at the end of the article



© The Author(s) 2025. **Open Access** This article is licensed under a Creative Commons Attribution-NonCommercial-NoDerivatives 4.0 International License, which permits any non-commercial use, sharing, distribution and reproduction in any medium or format, as long as you give appropriate credit to the original author(s) and the source, provide a link to the Creative Commons licence, and indicate if you modified the licensed material. You do not have permission under this licence to share adapted material derived from this article or parts of it. The images or other third party material in this article are included in the article's Creative Commons licence, unless indicated otherwise in a credit line to the material. If material is not included in the article's Creative Commons licence and your intended use is not permitted by statutory regulation or exceeds the permitted use, you will need to obtain permission directly from the copyright holder. To view a copy of this licence, visit <http://creativecommons.org/licenses/by-nc-nd/4.0/>.

Graphic Abstract



Keywords Cervical cancer, Apoptotic tumor cell-derived extracellular vesicles (apoEVs), MTA1, Tumor dormancy, Radioresistance

Introduction

Cervical cancer (CC) ranks as the most prevalent gynecologic cancer worldwide, posing a serious health risk to women [1]. Radiotherapy plays a crucial role as an adjunctive treatment for CC, helping to improve survival rates in early-stage patients and decrease recurrence in those with advanced disease. However, obstacles such as resistance to radiation and radiation-induced bystander effects (RIBEs) present significant challenges, impeding effective CC treatment and contributing to tumor relapse [2]. Consequently, understanding the mechanisms behind radioresistance is essential for developing novel therapeutic strategies to enhance treatment outcomes for patients with CC.

The rapid growth of tumors places significant stress on the tumor microenvironment, creating harsh conditions that lead to a combination of dying and dividing cells [3]. Recent studies suggest that signals from apoptotic cells may play a role in promoting cancer progression [4–5]. Clinically, data reveal a paradox where tumors

with higher levels of cell death often exhibit aggressive characteristics and are linked to poorer patient survival outcomes [6]. Various signaling pathways can facilitate communication between apoptotic and surviving tumor cells. A key example is extracellular vesicles (EVs), which apoptotic tumor cells release; these EVs are absorbed by nearby cells within the tumor microenvironment (TME), establishing what some describe as an “onco-regenerative niche” [7]. EVs, typically 30–200 nm in size, carry lipids, proteins, and nucleic acids, enabling them to mediate communication between cells. Proteins within EVs can act as signaling agents, inducing changes that support resistance to treatment and other functional adaptations triggered by cell death [8]. Metastasis-associated protein 1 (MTA1) is of particular interest for its multiple roles in cellular processes and cancer progression. It is also a stress-responsive protein that becomes upregulated under various stress conditions, including hypoxia, heat shock, and ionizing radiation [9]. Notably, MTA1 can be transported via EVs from breast cancer cells to

neighboring cells, influencing pathways that drive cancer progression [10]. Based on existing studies, we hypothesize that apoptotic EVs (apoEVs) may carry MTA1 to adjacent cervical cancer cells, potentially contributing to radioresistance. However, the precise mechanisms of communication between apoptotic and surviving tumor cells remain unclear.

Cellular dormancy, where cells remain in a non-proliferative state arrested in the G0-G1 phase, is recognized as a key contributor to resistance against therapy [11]. Dormant tumor cells, which exhibit traits like reduced sensitivity to treatments and immune evasion, are often considered the “seeds” of relapse and metastatic spread [12]. Therefore, targeting these dormant cells is seen as a promising strategy for reducing cancer recurrence. The TME, with factors like increased oxidative stress and signaling molecules (e.g., TGF β , BMP4, BMP7, IFN- γ), has been implicated in inducing dormancy in solid tumors [13]. Nonetheless, the specific mechanisms by which tumor cells respond to signals from the TME to initiate and sustain dormancy remain largely uncharted. Recent research has underscored the role of an apoptosis-driven “onco-regenerative niche” in fostering cellular dormancy [14]. The interaction between apoptotic extracellular vesicles (apoEVs) and dormant cell states may offer a new perspective on the mechanisms underlying radioresistance. This study investigates the hypothesis that apoEV-MTA1 may shift the phenotype of surviving tumor cells toward dormancy, enhancing their resistance to radiation and potentially pointing to novel targets to improve radiosensitivity in clinical applications.

Materials and methods

Ethics statement

This study received approval from the Ethics Committee at the Third Affiliated Hospital of Southern Medical University (Approval No. 2023-021). Given that it relied on leftover specimens and standard medical records, informed consent was waived. Animal research was performed in accordance with the Guidelines for the Care and Use of Laboratory Animals and was authorized by the Institutional Review Board of Nanfang Hospital, Southern Medical University (Approval No. NFYY-2022-0219).

Cell culture and clinical specimens

Human cervical cancer (CC) cell lines (SiHa and HeLa) were sourced from the American Type Culture Collection (ATCC, USA) and cultured according to the manufacturer’s guidelines. Additionally, 20 archived formalin-fixed, paraffin-embedded CC tissue samples were obtained from voluntary patients at the Gynecological Oncology Department of the Third Affiliated Hospital, Southern Medical University, who had not received

radiotherapy or chemotherapy before surgery in 2018. These samples included 10 radiosensitive and 10 radioresistant cases. In 2021, fresh cervical cancer tissues were also collected from six patients who underwent abdominal radical hysterectomy without prior radiation or chemotherapy at the same institution. Each sample was reviewed independently by two pathologists, with clinicopathological information anonymized. Supplementary Table 1 provides detailed patient data.

EV isolation, characterisation, and treatment

Extracellular vesicles (EVs) were isolated from the supernatant of cervical cancer cell cultures through ultracentrifugation. Initially, cells were removed by centrifuging at 1,000 g for 10 min. The resulting supernatant was filtered using a 0.8 μ m Millipore filter (USA). EVs were then collected by centrifuging at 120,000 g for 70 min at 4 °C. The EV pellet was resuspended in 100 μ l of PBS for further applications, including morphological analysis via transmission electron microscopy (TEM), size distribution using Nanosight particle tracking analysis (NTA), protein profiling, in vitro treatments, and in vivo experiments. For TEM, EVs were fixed with 2% glutaraldehyde, placed on carbon-coated grids, and negatively stained with phosphotungstic acid for 2 min before imaging with a TEM system (Hitachi H-7500, Japan). To study EV uptake, EVs were incubated for 20 min with 1 μ M PKH67 membrane dye (Sigma, USA), followed by washing to remove unbound dye. The labeled EVs were resuspended and co-cultured with CC cells. For in vitro studies, EV pellets were diluted in fresh culture medium to a final concentration of 50 μ g/ml, a level reflecting the clinically relevant range of EV concentrations in the blood of cancer patients (20–100 μ g/ml) [15]. For in vivo experiments, EV pellets were suspended in PBS and administered at 15 μ g per mouse via injection [16]. To standardize EV quantities across samples, total protein content was measured using the bicinchoninic acid (BCA) protein assay.

Irradiation in vitro

Cells from each group were seeded into disposable T25 culture flasks at a density of 5×10^6 cells per flask and incubated under standard conditions of 5% CO $_2$ at 37 °C for 24 h. Prior to radiation exposure, the flasks were filled with culture medium, and a condenser plate was used to ensure a consistent medium thickness of 1.5 cm. The cells were irradiated with a total dose of 16 Gy at a rate of 1 Gy per minute using a medical electron linear accelerator. The source-to-axis distance was maintained at 100 cm. After irradiation, the cells were cultured for an additional 48 h.

Colony formation assay

Cells were plated in six-well plates at varying densities (1,000, 2,000, 4,000, or 6,000 cells per well) and exposed to different doses of ionizing radiation (0, 2, 4, or 6 Gy) for 24 h. After a 14-day incubation period, the cells were fixed with 10% paraformaldehyde and stained using a 1x Giemsa solution (LEGANE, Beijing, China). Colonies containing at least 50 cells were counted. Plating efficiency (PE) was calculated as follows: $PE = (\text{number of colonies formed} / \text{number of cells initially seeded}) \times 100\%$. The surviving fraction was determined by dividing the PE of irradiated cells by the PE of control cells. This parameter is widely used as an indicator of radiosensitivity [17].

Glucose consumption

Cells were collected and lysed for 10 min at room temperature (24 °C), then incubated for 30 min at 37 °C using the Glucose Oxidase Method Kit (#A154-1-1, Jiancheng, China). Absorbance was measured at 550 nm, and glucose consumption was determined based on a standard curve.

Apoptosis analysis

Apoptosis was assessed using the Annexin V-FITC Apoptosis Detection Kit (#KGA107, KeyGEN, China). Both adherent and suspended cells were harvested and resuspended in 195 μ l of Annexin V-FITC binding buffer. Next, 5 μ l of Annexin V-FITC and 10 μ l of propidium iodide (PI) solution were added. The mixture was gently agitated and incubated in the dark at room temperature for 15 min. The percentage of apoptotic cells was then analyzed using flow cytometry (BD FACSCanto™II System, USA).

Western blot

Proteins from cells and EVs were extracted using RIPA buffer supplemented with a 1x protease inhibitor cocktail. Around 50 μ g of protein was loaded onto a 10% SDS-PAGE gel for separation, transferred onto a PVDF membrane, and analyzed with specific antibodies. These included MTA1 (#ab71153, Abcam), QRICH1 (#ab241574, Abcam), ATF4 (#ab85049, Abcam), HSP70 (#4876, CST), TSG101 (#72312, CST), CD63 (#52090, CST), Calnexin (#2679, CST), Nuclease Receptor Subfamily 2 Group F member 1 (NR2F1) (#ab181137, Abcam), STAT1 (#14994, CST), p-STAT1 (#9167, CST), p38 (#8690, CST), p-p38 (#4511, CST), AKT (#4685, CST), p-AKT (#4060, CST), ERK (#4695, CST), p-ERK (#4370, CST), and GAPDH (#2118, CST).

Chromatin Immunoprecipitation (ChIP) assay

Cells were treated with 1% formaldehyde for cross-linking, followed by quenching with a glycine solution. A ChIP assay was performed using the Enzymatic ChIP Kit

(#9003, CST) according to the manufacturer's protocol. Immunoprecipitation was carried out with anti-STAT1 (#14994, CST) and control IgG (#2729, CST) antibodies. Enriched DNA fragments from the ChIP assay were analyzed using qPCR to detect STAT1-binding sites within the NR2F1 promoter region. Results were expressed as relative enrichment, normalized against the IgG control. Primer sequences used for ChIP-PCR are listed in Supplemental Table 2.

Dual luciferase reporter gene assay

The activity of STAT1-regulated genes in SiHa and HeLa cells was evaluated using dual-luciferase reporter assays, following the manufacturer's protocol [18]. Briefly, cells were co-transfected with either the STAT1 expression plasmid or the control vector pCDNA3.1(+), along with the pGL3-NR2F1 promoter construct (GeneChem Inc, China), using Lipofectamine™ 2000 (Invitrogen, USA). After 48 h, luciferase activity was measured using the Dual-Luciferase Reporter Assay System. All experiments were independently repeated three times. The cloning sequences can be found in Supplemental Table 3.

Immunohistochemistry

Immunohistochemistry was performed on 4 μ m sections obtained from formalin-fixed, paraffin-embedded xenograft tissues, using a streptavidin peroxidase kit (Beijing Zhongshan Biotechnology Co., China) according to the manufacturer's instructions. The sections were incubated with primary rabbit antibodies against Caspase-3 (#9661, CST), MTA1 (#ab71153, Abcam), and NR2F1 (#ab181137, Abcam). Visualization and imaging of the stained sections were carried out with an IX70 inverted fluorescence microscope (Olympus, Japan). Caspase-3, a key effector in the apoptotic pathway, is widely recognized as a molecular marker of apoptosis [19].

Animal experiments

Six-week-old nude mice (weighing 20–23 g) were obtained from the Experimental Animal Center of Southern Medical University (Guangzhou, China). The animal study was approved by the Animal Care Committee of Nanfang Hospital, Southern Medical University, following the Institutional Animal Care and Use Committee (IACUC) guidelines (Approval No. NFYY-2022-0219). A xenograft CSCC model was developed by injecting CC cells (SiHa/HeLa, 5×10^6) combined with 100 μ g of either shMTA1-apoEVs or NC-apoEVs into the flank region of each mouse ($n=3$ per group). Additionally, 15 μ g of EVs was administered directly into the tumor center every other day. Tumor dimensions (mm^3) were recorded every three days, and volumes were calculated using the formula: $\text{volume} = (\text{width}^2 \times \text{length}) / 2$. When the tumor size reached approximately 100 mm^3 , localized

X-ray irradiation was applied every two days (2 Gy per session, for a total of three sessions). Fourteen days after the final radiation treatment, mice were euthanized with a barbiturate overdose, and tumors were harvested for further analysis.

Statistical analysis

Data analysis was performed using SPSS software (version 20.0). The t-test or one-way ANOVA was applied to compare the results, while the chi-squared test was used for frequency analysis. Pearson's correlation coefficient was calculated to evaluate the relationships between categorical variables. All experiments were repeated three times, and data were presented as mean \pm standard deviation (SD). A P-value of less than 0.05 was considered statistically significant.

Results

MTA1 is highly expressed in apoptotic CC cells and correlates with radioresistance of CC patients

Radioresistance is a complex biological phenomenon influenced by multiple factors [20]. Recent studies indicate that aggressive tumors often contain both apoptotic and actively proliferating cells, with apoptotic cells playing a crucial role in tumor progression and treatment responses [21]. To investigate the presence of apoptotic cells in cervical cancer (CC), we analyzed caspase-3 activity in six freshly obtained CC patient samples. Flow cytometry revealed that apoptotic cells represented 8–50% of the total tumor cells (Fig. 1A). To explore the impact of these cells on neighboring “healthy” tumor cells, we used mouse CC xenograft models. A mixture of lethally irradiated and untreated SiHa or HeLa cells was implanted into the flanks of immunocompromised mice, with a control group receiving only untreated tumor cells. Tumor growth and survival analysis showed that the co-injection of apoptotic CC cells with live tumor cells promoted tumor growth and radioresistance, leading to poorer prognosis in the mice (Fig. S1). These findings suggest that apoptotic cells present in tumors may play a significant role in regulating radioresistance.

Next, we performed bioinformatics analysis on the publicly available GSE236738 dataset, separating the samples into radiotherapy-sensitive and resistant groups. Twelve differentially expressed genes were identified using the criteria of “ $P < 0.05$, fold change > 10 ” (Supplementary Table 4). Functional enrichment and protein interaction analysis via KEGG, Metascape, and STRING platforms (Fig. 1B–C) highlighted a strong involvement of the cell stress signaling pathway. MTA1, QRICH1, and ATF4 emerged as key players, all stress-responsive proteins that are upregulated in response to various stressors, including heat shock, hypoxia, and radiation, and regulate gene expression. RT-qPCR and Western blot

analysis further confirmed a significant increase in MTA1 expression in radioresistant samples (Fig. 1D–E). Additionally, higher MTA1 expression was associated with reduced overall survival in CC patients based on TCGA data (Fig. 1F, cutoff: 7.67, $P = 0.0319$). IHC staining of tissues from 20 CC patients before radiotherapy revealed intense MTA1 staining in apoptotic tumor regions, where caspase-3 was abundantly expressed. In contrast, MTA1 levels were lower in caspase-3-deficient, non-apoptotic areas. Statistical analysis showed significantly higher levels of caspase-3 and MTA1 in radioresistant tissues compared to sensitive tissues (Fig. 1H, $P < 0.05$). Pearson's correlation analysis demonstrated a significant association between caspase-3 and MTA1 (Fig. 1I, $r = 0.6870$, $P < 0.001$). Together, these results indicate that MTA1 is highly expressed in apoptotic CC cells and strongly correlates with radioresistance and poor patient outcomes.

EVs secreted by apoptotic CC cells confer radioresistance of recipient CC cells

Apoptosis in cervical cancer (CC) cells was triggered by exposure to 16 Gy γ -irradiation (IR) (Fig. 2A). Following this, we incubated the CC cells with conditioned medium (CM) from apoptotic cells. Flow cytometry and colony formation assays showed that factors secreted by apoptotic CC cells exhibited an anti-apoptotic effect, thereby enhancing the radioresistance of healthy CC cells (Fig. S2). Notably, this effect was neutralized when CM was filtered to remove EVs, suggesting that EVs play a role in mediating the influence of apoptotic cells (Fig. S2). We then isolated and purified the EVs from the cell culture supernatants using ultracentrifugation. The characteristics, such as size, shape, and number of isolated EVs, were confirmed by TEM and NTA. TEM revealed that the vesicles had a round or oval shape with a disc-like structure and intact membrane (Fig. 2B). NTA analysis indicated a noticeable increase in the quantity and size of EVs released from CC cells following apoptosis induction (Fig. 2C). Western blotting showed that the isolated EVs expressed surface markers such as CD63, heat shock protein 70 (HSP70), and tumor susceptibility gene 101 (TSG101), while the negative marker Calnexin was expressed at low levels (Fig. 2D), confirming successful isolation. Moreover, MTA1, a factor associated with apoptosis, was significantly elevated in the apoEVs (Fig. 2D). The uptake of EVs by CC cells was monitored using laser confocal microscopy. No fluorescence was observed in the PBS-treated group, whereas green fluorescence was seen in the cytoplasm of CC cells cocultured with either apoEVs or ncEVs (Fig. 2E), with no significant difference in fluorescence intensity between the two groups ($P > 0.05$; Fig. 2F). Furthermore, CC cells exposed to apoEVs showed an increase in MTA1 expression compared to cells treated with ncEVs (Fig. 2G). To

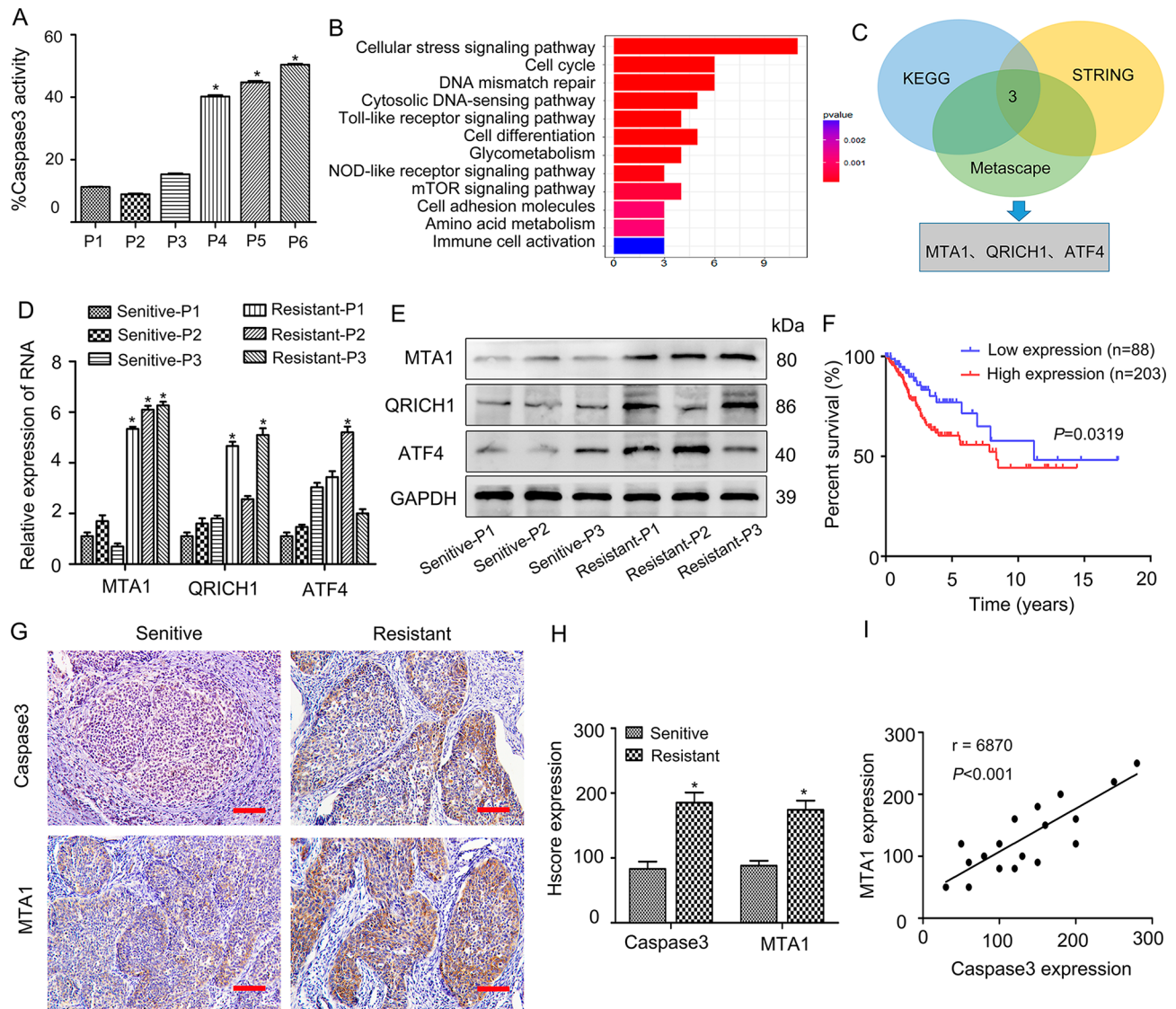


Fig. 1 MTA1 is highly expressed in apoptotic CC cells and correlates with radioresistance of CC patients. **(A)** Assessment of caspase-3 activity using FACS analysis in six freshly dissociated tumor samples. **(B)** Gene ontology enrichment analysis of 12 differentially expressed genes from the GSE236738 public dataset. **(C)** Identification of MTA1, QRICH1, and ATF4 as potential radioresistance regulators through Venn diagram analysis across KEGG, Metascape, and STRING platforms. **(D)** RT-qPCR analysis comparing the RNA expression levels of MTA1, QRICH1, and ATF4 in radiotherapy-sensitive and resistant CC tissues. **(E)** Western blot analysis showing the protein expression levels of MTA1, QRICH1, and ATF4 in radiotherapy-sensitive and resistant CC tissues. **(F)** TCGA data indicating that MTA1 overexpression is associated with poor prognosis in CC patients ($*P=0.0319$, log-rank test). **(G)** Representative IHC staining images of caspase-3 and MTA1 in radiotherapy-sensitive and resistant CC tissues at 200x magnification (scale bar, 50 μm). **(H)** Statistical analysis of caspase-3 and MTA1 expression levels ($*P < 0.05$). **(I)** Pearson correlation analysis showing a significant clinical correlation between caspase-3 and MTA1 ($r=0.6870$, $P < 0.001$).

investigate the impact of apoEVs on the phenotype of surviving CC cells, we co-cultured CC cells with either apoEVs or ncEVs and subjected them to irradiation. Flow cytometry analysis (Fig. 2H) and colony formation assays (Fig. 2I-J) demonstrated that CC cells co-cultured with apoEVs exhibited reduced apoptosis and enhanced colony formation compared to cells co-cultured with ncEVs ($P < 0.05$). Notably, the promoting effect of apoEVs was diminished when the EV donor cells were pre-treated with the caspase inhibitor zVAD(OMe)fmk (Fig. S3).

To verify these findings *in vivo*, we analyzed xenograft tumors from mice injected with luciferase-labeled SiHa or HeLa cells, along with EVs derived from either lethally irradiated (apoEVs) or untreated (ncEVs) cells. The *in vivo* data also confirmed the radioresistance-inducing effect of apoEVs (Fig. S4). These results further support the hypothesis that MTA1 secreted by apoptotic cells may help neighboring cells withstand subsequent stressors and enhance their resistance to therapy.

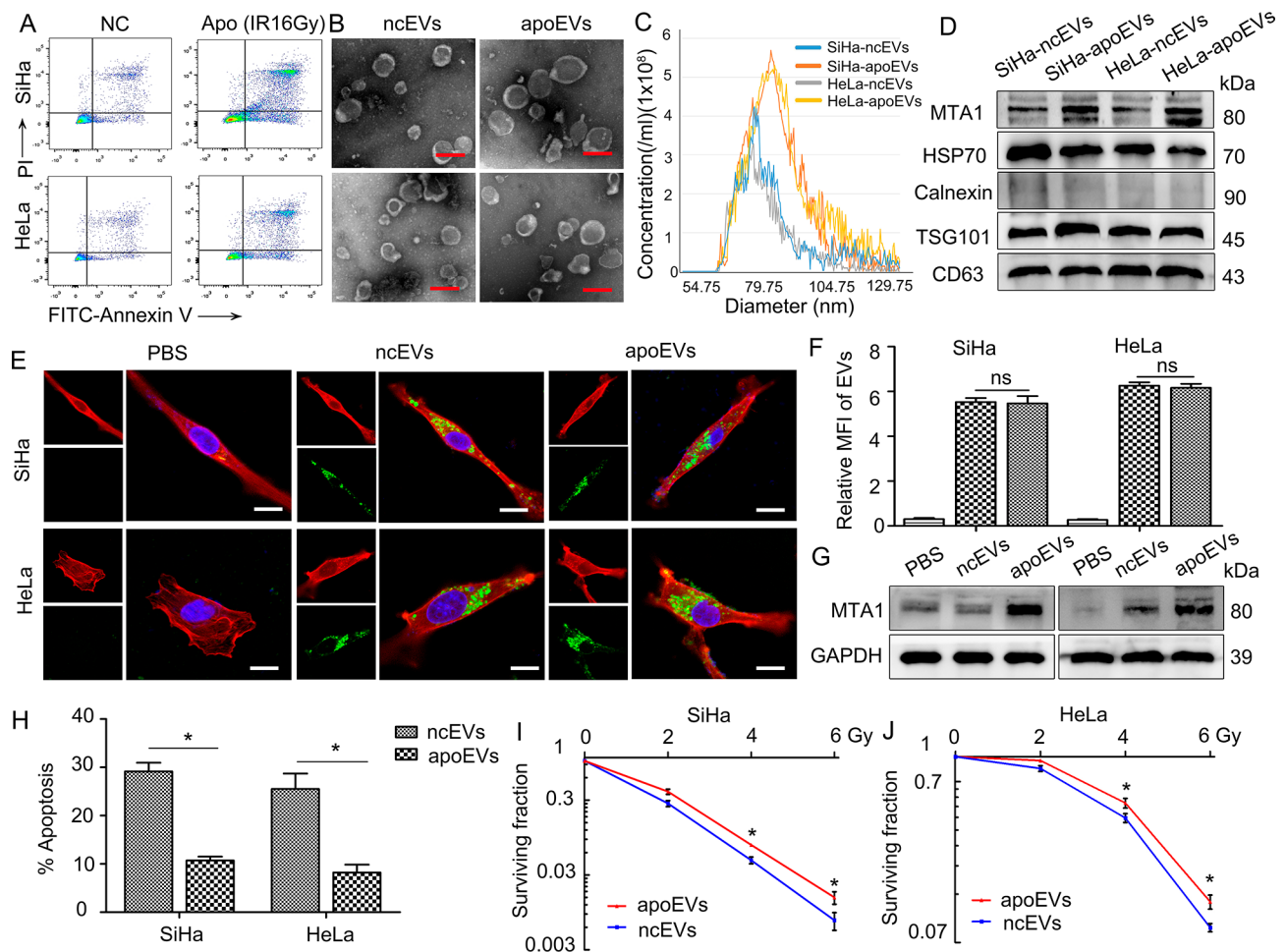


Fig. 2 EVs secreted by apoptotic CC cells confer radioresistance of recipient CC cells. **(A)** FACS analysis for Annexin V/PI staining of SiHa and HeLa cells, comparing untreated (NC) with those exposed to 16 Gy lethal irradiation (Apo). **(B)** Transmission electron microscopy (TEM) was used to confirm the morphology of EVs secreted by untreated (ncEVs) or irradiated (apoEVs) SiHa and HeLa cells. Scale bar: 100 nm. **(C)** Nanoparticle tracking analysis (NTA) to measure the EVs produced by untreated or irradiated SiHa and HeLa cells. **(D)** Western blotting to validate the presence of EV markers (HSP70, TSG101, CD63), absence of the EV exclusion marker Calnexin, and detection of MTA1 expression. **(E)** Confocal microscopy images of SiHa and HeLa cells treated with PKH67-labeled EVs (green) from untreated or irradiated CC cells, with phalloidin (red) and DAPI (blue) staining. Scale bar: 20 μ m. **(F)** Mean fluorescence intensity (MFI) analysis revealing differences in EV uptake by recipient cells as shown in **(E)**. No significant difference (ns) was observed. **(G)** MTA1 levels in SiHa and HeLa cells treated with indicated EVs or PBS for 48 h, analyzed by Western blot. **(H)** FACS analysis for Annexin V/PI staining of SiHa and HeLa cells exposed to ncEVs or apoEVs. Colony formation assays assessed radiation sensitivity. apoEVs enhanced clonogenic survival in SiHa **(I)** and HeLa **(J)** cells compared to ncEVs (* $P < 0.05$)

MTA1 is exported from apoptotic cells in a caspase dependent manner

Under typical physiological conditions, MTA1 is mainly found in the nucleus. This raises the question of how MTA1 shifts to EVs following the induction of apoptosis. To investigate this, we performed co-transfection experiments in CC cells using plasmids encoding GFP-tagged MTA1 and RFP-tagged scaffold protein Coilin. Apoptosis was induced by radiation (16 Gy) 24 h after transfection, resulting in the dissociation of MTA1 from Coilin and its subsequent translocation to the cytoplasm (Fig. 3A). Additionally, we detected cytoplasmic MTA1 localization in CC cells that also exhibited positive staining for phospho-H2AX, which marks DNA damage and the early

stages of apoptosis (Fig. 3B) [22]. To determine if MTA1 is specifically exported to the cytoplasm or if its translocation is simply due to nuclear envelope breakdown, we co-transfected CC cells with plasmids encoding GFP-tagged MTA1 and RFP carrying a nuclear localization signal (RFP-NLS). During both early and late stages of apoptosis, both MTA1 and NLS moved to the cytoplasm, while at the non-apoptotic stage, they remained predominantly in the nucleus (Fig. 3C). Furthermore, we examined the role of caspases in MTA1's cytoplasmic export. The export of MTA1 via apoEVs was blocked by the caspase inhibitor zVAD(OMe)fmk, indicating that this process is dependent on caspase activity (Fig. 3D). Caspases are critical in cleaving various proteins during early

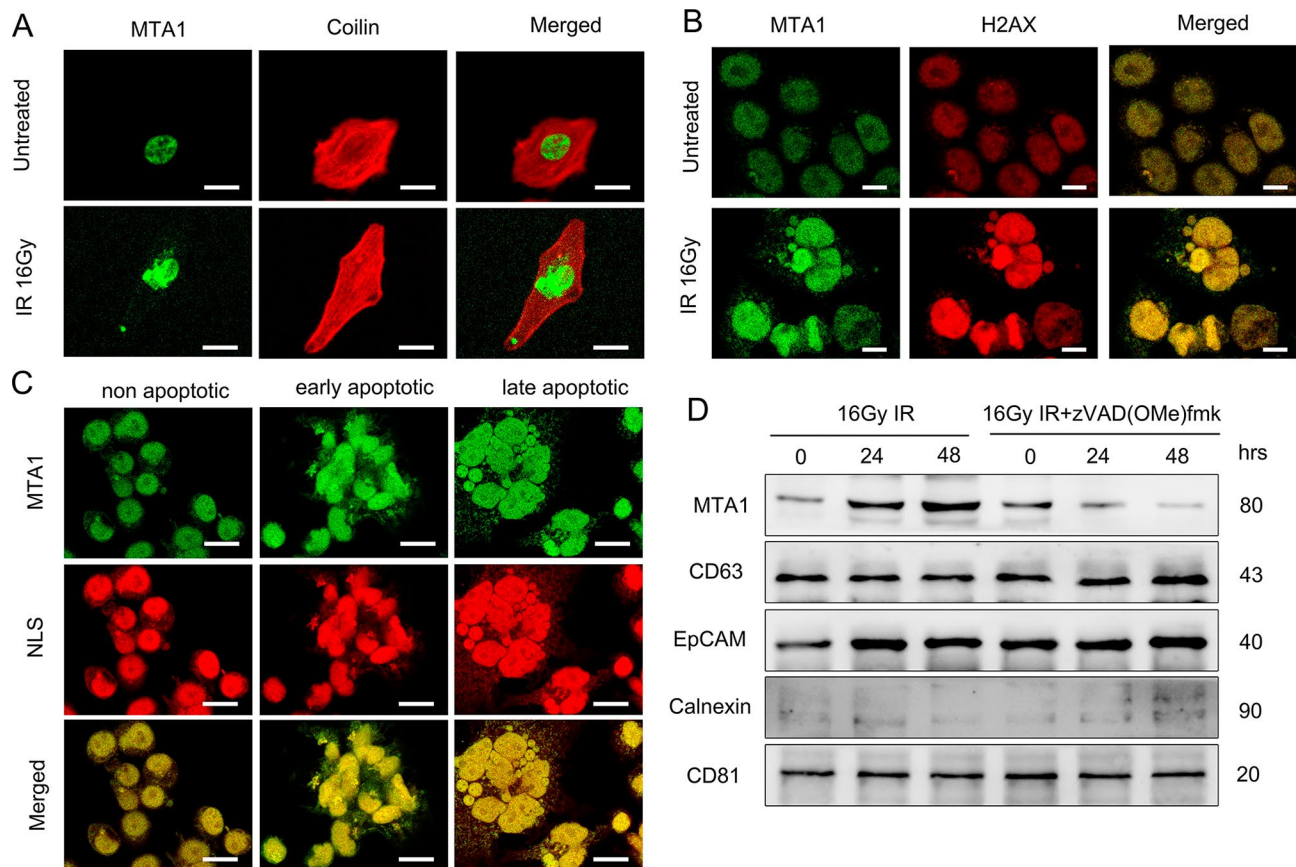


Fig. 3 MTA1 is exported from apoptotic cells in a caspase dependent manner. **(A)** Fluorescence microscopy images showing SiHa cells co-expressing GFP-MTA1 and RFP-Coilin, taken 24 h after 16 Gy lethal irradiation (IR). **(B)** Immunofluorescence staining of CC cells, with MTA1 labeled in green and phosphorylated histone H2AX in red. **(C)** Fluorescence images of CC cells co-expressing GFP-MTA1 and RFP-NLS following IR treatment. **(D)** Western blot analysis of EVs isolated from CC cells subjected to IR for different time points, with or without the pan-caspase inhibitor zVAD(OMe)fmk

apoptosis, which results in changes to their function and localization [23]. These findings suggest that the activation of caspase-3 could be a key mechanism facilitating the nuclear export of MTA1, which is then encapsulated in apoEVs.

apoEV-MTA1 promotes radioresistance by inducing cellular dormancy

We used lentiviral vectors to knock down MTA1 expression in SiHa and HeLa cells. MTA1 was found to be significantly enriched in EVs derived from apoptotic CC cells compared to EVs secreted by shMTA1 CC cells (Fig. 4A-B). To confirm the transfer of MTA1 through apoptotic EVs (apoEVs) to recipient cells, CC cells were treated with apoEVs for 24 h, resulting in a marked increase in intracellular MTA1 levels in the recipient cells (Fig. 4C). To investigate whether MTA1 was responsible for the phenotypic changes in recipient CC cells induced by apoEVs, we knocked down MTA1 in apoEVs and observed an increased apoptosis rate in recipient cells (Fig. 4D-E). Additionally, colony formation assays showed that MTA1-enriched apoEVs promoted radioresistance

in the recipient cells (Fig. 4F-G). Next, we assessed the influence of apoEVs on gene expression related to cellular dormancy in the recipient cells. After treating CC cells with either shMTA1-apoEVs or shNC-apoEVs, RNA and protein analyses revealed that shNC-apoEVs, but not shMTA1-apoEVs, significantly upregulated dormancy markers, especially NR2F1 (Fig. 4H-I). Inducing cell dormancy is known to involve the suppression of aerobic glycolysis, often referred to as the Warburg effect [24]. In line with this, we observed that CC cells treated with shNC-apoEVs exhibited a marked reduction in glycolysis compared to those treated with shMTA1-apoEVs (Fig. 4J). It is well-established that cells in dormancy are typically arrested in the G0/G1 phase of the cell cycle, making them less sensitive to radiation-induced damage [25]. Our results indicate that MTA1 acts as a key regulator of the cell cycle. The knockdown of MTA1 disrupted the G0/G1 phase arrest in recipient CC cells (Fig. 4K). These findings suggest that MTA1, when enriched in apoEVs, can enhance radioresistance by promoting G0/G1 phase arrest, a characteristic of cell dormancy. Thus, when CC cells undergo apoptosis, they paradoxically

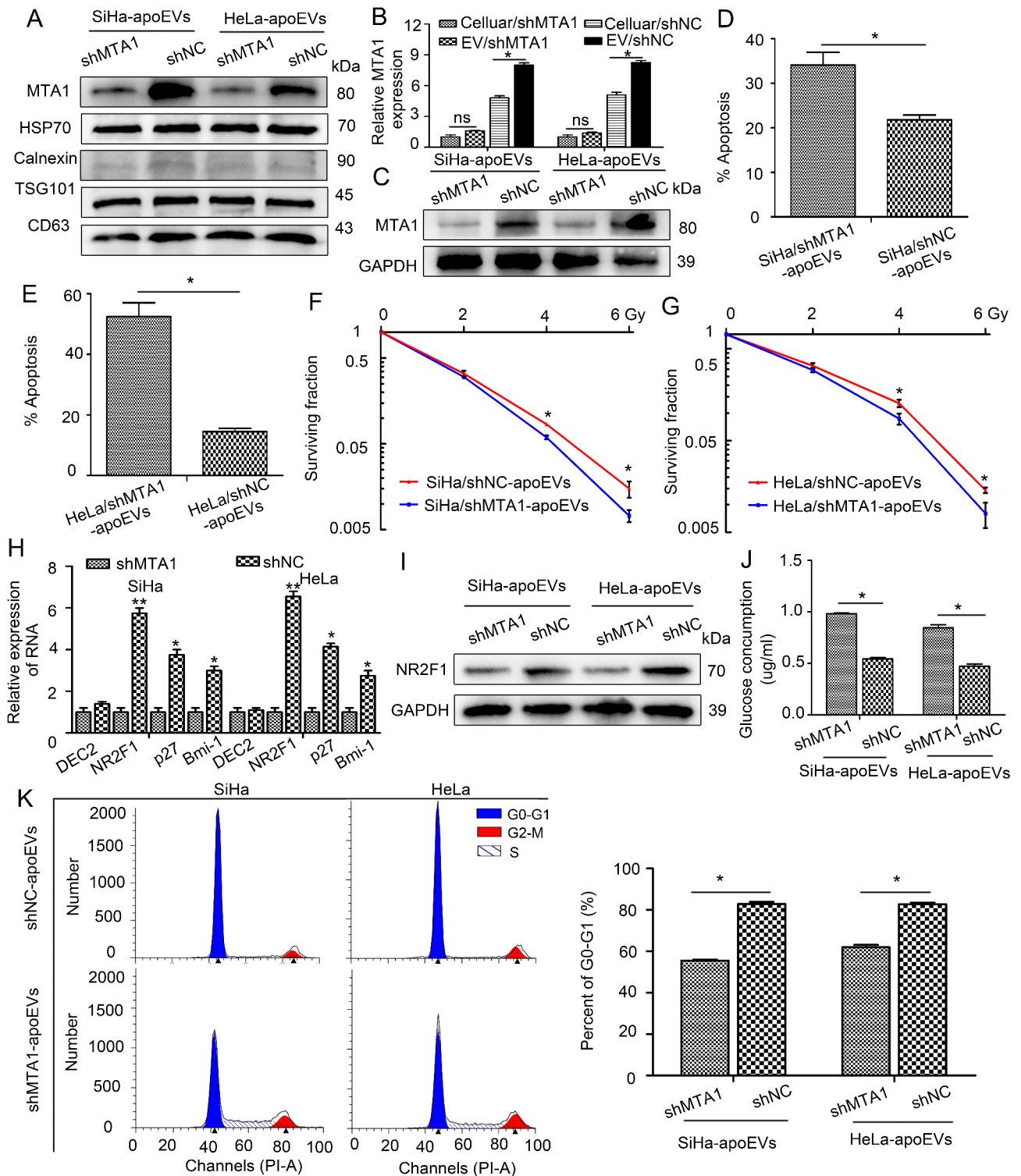


Fig. 4 apoEV-MTA1 promotes radioresistance by inducing cellular dormancy. **(A)** Western blot analysis assessing the expression levels of MTA1 in EVs from CC cells infected with either the MTA1 knockdown virus (shMTA1) or the control virus (shNC). **(B)** Grayscale analysis of MTA1 expression in the indicated cells and corresponding EVs using western blotting. * $P < 0.05$. ns, no significant difference. **(C)** Detection of MTA1 levels in CC cells after 48-hour pretreatment with the specified EVs, analyzed by western blot. **(D)** FACS analysis of Annexin V/PI staining in SiHa **(D)** and HeLa **(E)** cells treated with either shMTA1-apoEVs or shNC-apoEVs. Radiation sensitivity was assessed through colony formation assays. **(F)** Decreased clonogenic formation in SiHa and **(G)** HeLa cells treated with shMTA1-apoEVs compared to shNC-apoEVs. **(H)** qRT-PCR analysis of key dormancy regulators (DEC2, NR2F1, p27, Bim-1) in CC cells treated with either shMTA1-apoEVs or shNC-apoEVs. **(I)** Western blot analysis showing NR2F1 expression levels in CC cells after treatment with shMTA1-apoEVs or shNC-apoEVs. **(J)** Glucose consumption analysis in CC cells after incubation with shMTA1-apoEVs or shNC-apoEVs for 48 h. **(K)** FACS analysis of cell cycle progression in CC cells after 48-hour incubation with shMTA1-apoEVs or shNC-apoEVs

promote an anti-apoptotic effect and a dormancy phenotype in surviving cells, contributing to increased radioresistance.

STAT1 activation triggers NR2F1 expression to sustain dormancy

ApoEVs have the potential to activate several signaling pathways involved in tumor cell dormancy and radioresistance, including AKT, STAT1, P38 MAPK, and ERK pathways [26]. To pinpoint the primary signaling pathway responsible for the enhanced radioresistance mediated by apoEV-MTA1, we analyzed the activation of key signaling molecules in recipient cells treated with apoEV-MTA1. Our results showed a significant increase in phosphorylation of STAT1, while the levels of other signaling proteins remained largely unchanged (Fig. 5A). Notably, no activated STAT1 was detected in the apoEVs themselves (Fig. S5), indicating that the activation of STAT1 occurs in the recipient tumor cells and is not transferred via the EVs. These findings suggest that apoEVs promote p-STAT1 signaling by delivering MTA1 to the recipient cells. Furthermore, MTA1 was found to upregulate NR2F1 expression, an effect that was reversed by siSTAT1 (Fig. 5B). When we activated and inhibited p-STAT1 signaling using 2-NP and Fludarabine (F-ara-A), respectively, we observed notable increases and decreases in NR2F1 expression in the recipient cells (Fig. 5C). Bioinformatics analysis using the JASPAR database identified six potential STAT1 binding sites (SBSs) in the NR2F1 promoter region (Fig. 5D). Luciferase reporter assays showed increased luciferase activity driven by the NR2F1 promoter in cells with activated p-STAT1, while decreased activity was observed in p-STAT1 inhibited cells ($P < 0.05$; Fig. 5E). Additionally, ChIP assays confirmed that p-STAT1 binds to SBS1, SBS3, and SBS4 within the NR2F1 promoter region (Fig. 5F), further supporting the transcriptional upregulation of NR2F1 by p-STAT1.

We further examined how the apoEV-induced activation of p-STAT1 signaling contributes to radioresistance and whether inhibiting p-STAT1 could restore sensitivity of CC cells to radiotherapy. Inhibition of p-STAT1 significantly increased glycolysis in recipient cells treated with apoEVs (Fig. 5G, Fig. S6A). The suppression of G0/G1 phase arrest was more pronounced in cells with p-STAT1 inhibition than in the control group (Fig. 5H-I, Fig. S6B). Additionally, colony formation assays showed a marked reduction in colony numbers when p-STAT1 signaling was blocked in recipient cells treated with apoEVs (Fig. 5J, Fig. S6C), suggesting that inhibiting p-STAT1 activity can counteract the radioresistance induced by apoEVs. Similar findings were observed in apoptotic flow staining assays (Fig. 5K, Fig. S6D). Conversely, activating p-STAT1 expression reversed the radiosensitization effects seen with shMTA1-apoEVs. These results confirm

that p-STAT1 activation plays a critical role in the radioresistance promoted by apoEVs delivering MTA1 to recipient tumor cells.

apoEV-MTA1 promotes radioresistance of CC in vivo

To explore whether apoEVs carry MTA1 to modulate cell dormancy and influence radioresistance in vivo, nude mice were subcutaneously implanted with CC cells that had been cultured with serum-free medium containing either shMTA1-apoEVs or shNC-apoEVs and then exposed to radiation. Tumor growth was significantly greater in mice injected with CC cells treated with shNC-apoEVs compared to those treated with shMTA1-apoEVs (Fig. 6A, Fig. S7A). Moreover, survival times were shorter in the shNC-apoEV group than in the shMTA1-apoEV group (Fig. 6B, Fig. S7B). Western blotting (Fig. 6C, Fig. S7C) and IHC staining (Fig. 6D, Fig. S7D) showed that the expression of MTA1 and NR2F1 was notably higher in tumors from mice injected with CC cells transfected with shNC-apoEVs compared to those treated with shMTA1-apoEVs. These findings suggest that the overexpression of MTA1 in apoEVs promotes CC tumor growth in vivo by influencing cell dormancy.

Discussion

Recent studies have established the pivotal role of apoptotic cells in modulating tumor progression and therapeutic resistance [27]. Extending these findings, our study provides novel evidence that apoptotic tumor cells contribute to the development of radioresistance in neighboring surviving cells through the release of apoEVs. These apoEVs serve as critical mediators of intercellular communication, transferring functional molecular cargo that significantly influences tumor behavior and treatment response [28]. Of particular significance, we have identified MTA1 as a key molecular determinant within apoEVs that drives radioresistance through the induction of cellular dormancy. This discovery not only advances our understanding of radiation resistance mechanisms in CC but also establishes MTA1 as a potential therapeutic target for radiosensitization strategies, which may ultimately enhance the efficacy of radiotherapy in clinical settings.

Apoptosis, once considered a silent cell death process, is now recognized as a dynamic mechanism influencing intercellular communication and tissue remodeling [29]. In cancer, therapy-induced apoptotic cells paradoxically support the survival and growth of remaining tumor cells [5]. Our findings reveal that this “dying-for-surviving” mechanism is active in radiotherapy, where irradiated apoptotic cells release factors like PGE2 [4], HMGB1 [30], and VEGF [31] to promote angiogenesis, repopulation, and metastasis. apoEVs play a key role in therapy resistance, conveying molecular messages that

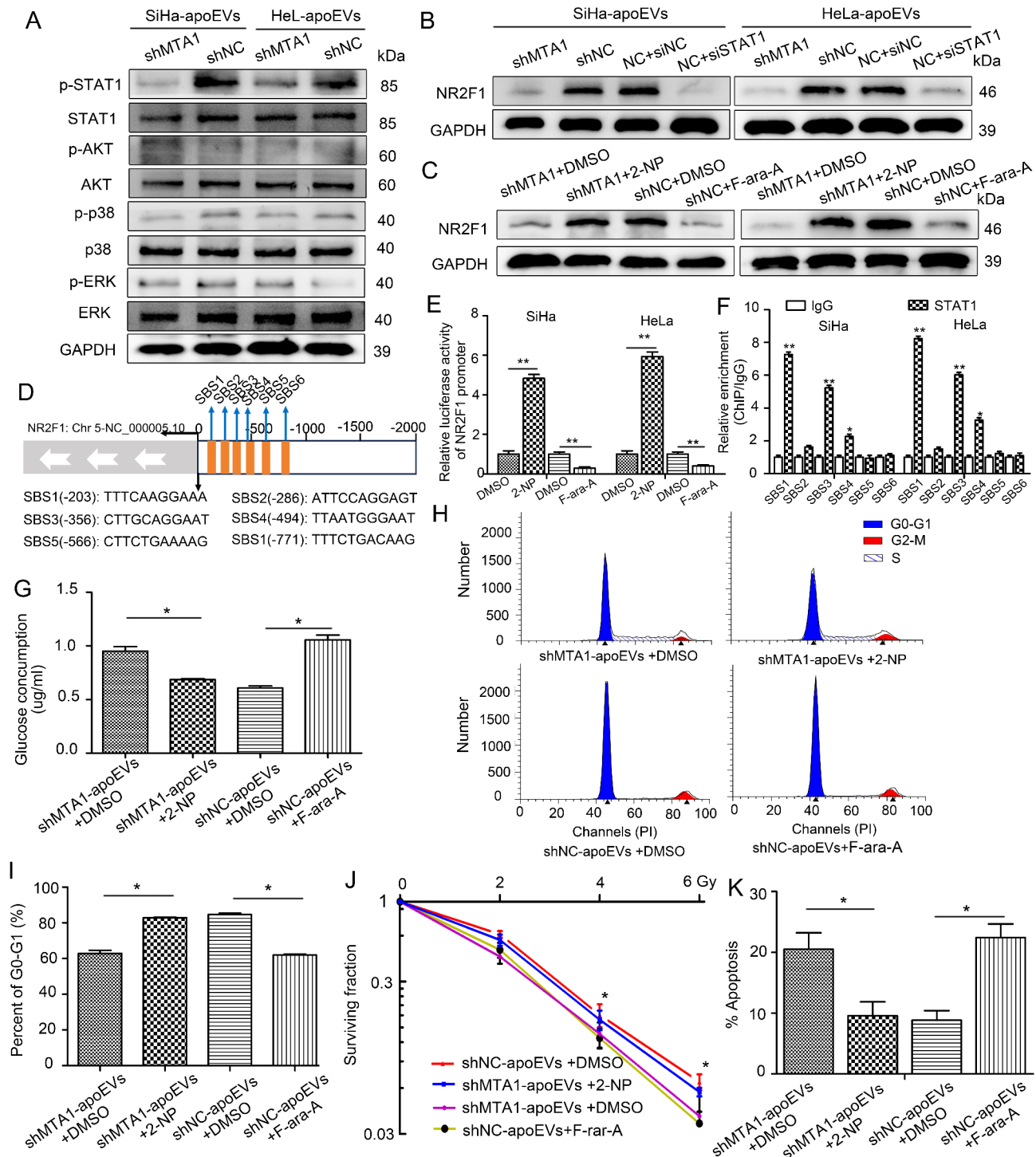


Fig. 5 STAT1 activation triggers NR2F1 expression to sustain dormancy. **(A)** Western blotting was used to assess downstream signaling pathways activated by apoEVs in CC cells. **(B)** NR2F1 protein expression was quantified in CC cells treated with shMTA1-apoEVs or shNC-apoEVs. Rescue experiments indicated that silencing STAT1 (siSTAT1) suppressed the increase in NR2F1 expression induced by shNC-apoEVs. **(C)** NR2F1 protein levels were measured in CC cells treated with 2-NP (a p-STAT1 activator) or F-ara-A (a p-STAT1 inhibitor) via western blotting. **(D)** A diagram showing the predicted STAT1 binding sites on the NR2F1 promoter. **(E)** Luciferase activity of the NR2F1 promoter was assessed in CC cells with either p-STAT1 activation or inhibition. **(F)** ChIP assays were conducted to examine STAT1 enrichment at the STAT1 binding sites (SBSs) in the NR2F1 promoter region, compared to IgG. **(G)** Glucose consumption was measured in SiHa cells incubated with the indicated EVs, along with 2-NP or F-ara-A, for 48 h. **(H-I)** Cell cycle progression was analyzed by FACS in SiHa cells treated with the indicated EVs and 2-NP or F-ara-A for 48 h. Radiation sensitivity was evaluated by colony formation assays **(J)** and apoptosis analysis **(K)**. Inhibition of p-STAT1 signaling significantly reduced colony formation and increased apoptosis in SiHa cells treated with apoEVs

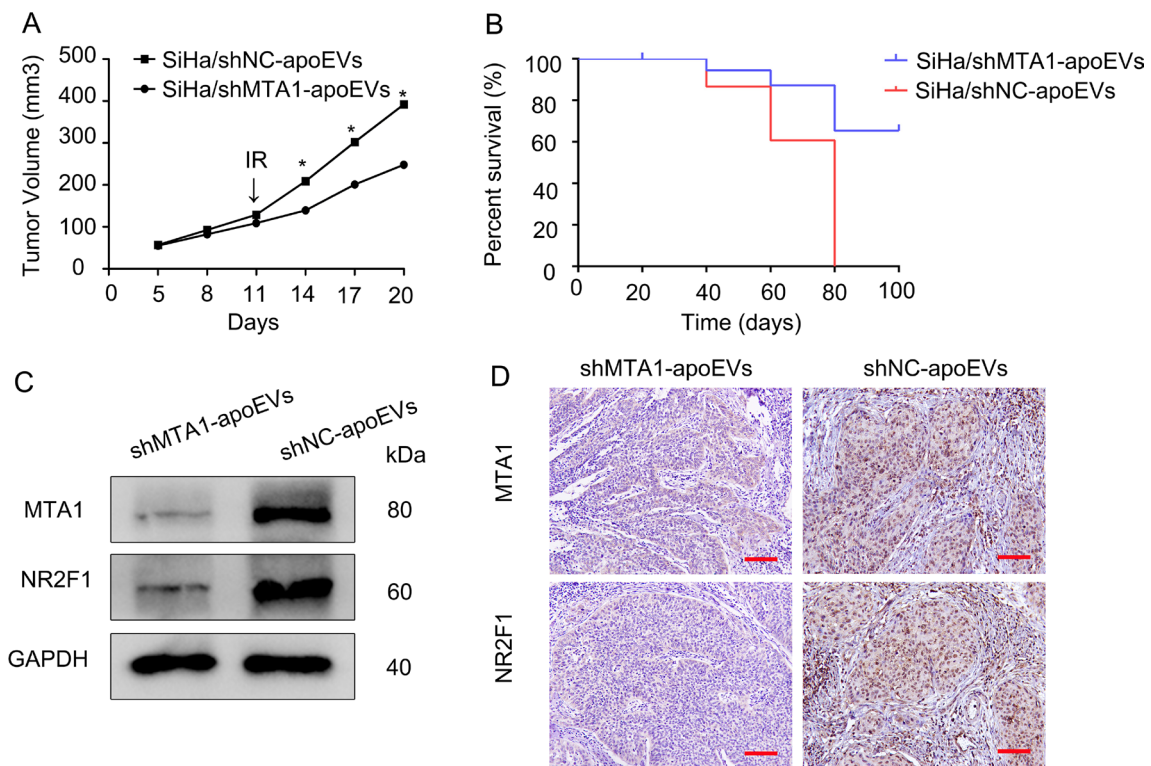


Fig. 6 apoEV-MTA1 promotes radioresistance of CC *in vivo*. **(A)** Tumor growth curves of the CC xenograft model *in vivo*. * $P < 0.05$. **(B)** Kaplan-Meier survival analysis of mice injected with SiHa cells treated with either shMTA1-apoEVs or shNC-apoEVs ($n = 3$ per group, $P < 0.05$, log-rank test). **(C)** Western blot results indicating the levels of MTA1 and NR2F1 expression in tumor tissue from each group of mice. **(D)** Representative IHC images showing the expression levels of MTA1 and NR2F1 in tumor sections from each group, with images captured at 200 \times magnification and a scale bar of 50 μm

influence surviving cells [32, 33]. ApoEVs also interact with immune cells: macrophages engulf apoEVs via surface proteins like CX3CL1 and ICAM-3 [34], but in cancer, apoEVs carrying immunosuppressive molecules (e.g., TGF- β , PD-L1) polarize macrophages toward an M2-like phenotype, fostering an immunosuppressive TME [35]. ApoEVs can impair dendritic cell (DC) antigen presentation, reducing T cell activation, yet they may also carry tumor antigens to stimulate DC-mediated T cell responses, offering potential for immunotherapy [36]. These dual roles highlight the complexity of apoEV-immune interactions in tumor progression. Our study shows that apoEVs from irradiated CC cells transfer MTA1, a metastasis-associated protein, to recipient cells, promoting radioresistance. MTA1, linked to poor prognosis in various cancers [37], stabilizes HIF-1 α under hypoxia to enhance angiogenesis and metabolic adaptation [38] and interacts with mitochondrial ATP5A to drive metabolic reprogramming and metastasis [39]. It also accumulates at DNA damage sites [40] and is highly expressed under stress [41], underscoring its role in therapy resistance. Upon internalization, apoEV-derived MTA1 avoids lysosomal degradation, translocates to the nucleus, and triggers a positive feedback loop that amplifies its effects, promoting a more malignant phenotype.

Targeting apoEV-MTA1 signaling holds promise for overcoming radioresistance, but challenges remain, including the specificity of apoEV-MTA1 uptake, and potential off-target effects due to MTA1's involvement in diverse cellular processes.

Despite growing research on MTA1, its role in treatment resistance remains poorly understood. A key mechanism underlying resistance is cancer cell dormancy, where cells enter a reversible G0 phase, enabling survival in hostile environments, evasion of immune detection [42]. For instance, dormant glioblastoma cells drive tumor recurrence after temozolomide chemotherapy [43], highlighting the need to target dormancy. Among dormancy regulators, NR2F1, a member of the steroid/thyroid hormone receptor superfamily, plays a central role. Our findings show that NR2F1 is silenced in proliferating CC cells but upregulated in dormant cells, initiating a dormancy gene signature. This includes SOX9, RAR β , and CDK inhibitors like p27 and p16, which induce G0/G1 arrest and quiescence [44]. NR2F1 also antagonizes MYC signaling, reducing proliferation and creating "immune cold" tumors with low mutation burden, homologous recombination deficiency (HRD), and minimal immune infiltration [45, 46]. Furthermore, NR2F1 triggers global chromatin repression and

maintains dormancy in disseminated tumor cells (DTCs) in the bone marrow, a process reversible through NR2F1 knockdown [47]. While targeting tumor dormancy is not yet a clinical reality, the regulation of NR2F1 offers promising therapeutic potential for clinical applications [48, 49]. Future research should develop NR2F1 inhibitors to disrupt its interaction with dormancy-associated pathways.

Cellular dormancy is regulated by a network of signaling pathways, including ERK/p38, SMAD1/5, TGF- β , and STAT1 [50, 51]. For instance, p38 regulates a gene network in head and neck squamous cell carcinoma (HNSCC) that promotes dormancy [52], while TGF- β 2 signaling via p38 α / β modulates disseminated tumor cell (DTC) dormancy and metastatic microenvironments [53]. Despite these insights, the link between dormancy and treatment resistance remains unclear. Our study reveals that apoEV-MTA1 triggers a STAT1-dependent signaling cascade, activating NR2F1 to sustain dormancy and create an “onco-regenerative niche” that supports tumor survival under stress. While STAT1 has been linked to post-dormancy growth [54], our findings highlight its role in maintaining dormancy via NR2F1 activation, potentially synergizing with other dormancy signals like TGF- β 2 and retinoic acid pathways. Targeting the apoEV-MTA1/p-STAT1/NR2F1 pathway offers therapeutic potential, but the reversibility of dormancy poses a risk of tumor recurrence. Combining STAT1 inhibition with immune checkpoint blockade may help overcome dormancy-mediated resistance.

Our findings have important clinical implications, potentially leading to new therapeutic approaches to reduce radioresistance and offering a novel biomarker for predicting tumor recurrence. Although MTA1 is a promising target for drug development due to its various roles, there is currently no drug specifically designed to target it. However, compounds that disrupt MTA1 interactions with key partners, such as histone deacetylase 1 (HDAC-1), have shown effectiveness in reducing metastasis and MTA1 expression in both cancer cell lines and animal models [55, 56]. Future research should focus on identifying small molecules or peptides that selectively disrupt MTA1’s oncogenic functions without affecting its physiological roles. Liquid biopsy is gaining traction for monitoring treatment responses and predicting outcomes in solid tumors [57]. Notably, EVs containing proteins are stable in plasma and show promise as cancer biomarkers. Unlike conventional methods such as IHC, plasma EVs provide a more accessible means of assessing the effects of the TME on cellular functions [58]. While MTA1 in apoEVs shows promise as a biomarker, large-scale clinical studies are needed to validate its sensitivity, specificity, and utility across different cancer types and treatment regimens.

Conclusion

This study highlights the importance of apoptotic TME signaling in cancer progression. We identify MTA1 as a nuclear factor transferred via apoEVs, revealing its role in promoting tumor dormancy and radioresistance in CC. Mechanistically, apoEV-MTA1 activates the p-STAT1/NR2F1 axis, establishing a pro-survival “onco-regenerative niche” that drives therapeutic resistance. Targeting the MTA1/p-STAT1/NR2F1 pathway offers a promising strategy to overcome radioresistance. Future studies should validate these findings in preclinical models, develop MTA1-specific inhibitors, and explore MTA1 in apoEVs as a predictive biomarker. This work advances our understanding of apoptotic signaling and opens new therapeutic avenues.

Abbreviations

CC	Cervical Cancer;
apoEVs	Apoptotic Tumor Cells-Derived EVs
RIBEs	Radiation-Induced Bystander Effects
EVs	Extracellular Vesicles
TME	Tumor Microenvironment
MTA1	Metastasis-associated protein 1
ATCC	American Type Culture Collection
BCA	Bicinchoninic Acid
TEM	Transmission Electron Microscopy
NR2F1	Nuclear Receptor Subfamily 2 Group F member 1
NTA	Nanosight particle Tracking Analysis
PI	Propidium Iodide
IACUC	Institutional Animal Care and Use Committee
SD	Standard Deviation
HRD	Homologous Recombination Deficiency
DTCs	Disseminated Tumor Cells
HDAC-1	Histone Deacetylase 1
HNSCC	Head and Neck Squamous Cell Carcinoma
RAR β	Retinoic Acid Receptor β

Supplementary Information

The online version contains supplementary material available at <https://doi.org/10.1186/s12967-025-06350-4>.

Supplementary Material 1

Acknowledgements

Not applicable.

Author contributions

CXJ and GSQ conceived and designed the study, DYR and WQZ wrote the initial draft of the manuscript. DRY, WQZ, ZW, CXJ, JHP, XCQ, CSC and FJ performed the experiments, analyzed the data, and assisted in manuscript preparation. All authors contributed to data collection, interpretation, and critical review of the manuscript. All authors approved the final version of the manuscript, and agree to be accountable for all aspects of the study.

Funding

This work was supported by the National Natural Science Foundation of China (Nos. 82002743; 82101704).

Data availability

All data generated or analyzed during this study are included in this published article.

Declarations

Ethics approval and consent to participate

The study was approved by the Ethics Committee of the Third Affiliated Hospital, Southern Medical University (No. 2023-021). As the specimens involved in the study came from residual specimens and routine medical records, our study met the requirement of informed consent exemption. Animal experiments were carried out in accordance with the Guidelines for the Care and Use of Laboratory Animals and approved by the Institutional Review Board of Nanfang Hospital, Southern Medical University (No. NFYY-2022-0219).

Consent for publication

Not applicable.

Competing interests

The authors declare that they have no competing interests.

Author details

¹Department of Obstetrics and Gynecology, The Third Affiliated Hospital, Southern Medical University, 183 Zhongshan Avenue West, Tianhe District, Guangzhou 510630, P.R. China

²Department of Radiation Oncology, Nanfang Hospital, Southern Medical University, Guangzhou 510515, China

³Department of Radiation Oncology, The Tenth Affiliated Hospital of Southern Medical University (Dongguan People's Hospital), Dongguan 523059, China

⁴Department of Gynecology, Guangdong Provincial People's Hospital (Guangdong Academy of Medical Sciences), Southern Medical University, 106 Zhongshan 2nd Road, Yuexiu District, Guangzhou 510080, P.R. China

Received: 18 January 2025 / Accepted: 3 March 2025

Published online: 14 March 2025

References

1. Vu M, Yu J, Awolude OA, Chuang L. Cervical cancer worldwide. *Curr Probl Cancer*. 2018;42(5):457–65.
2. Chargari C, Peignaux K, Escande A, Renard S, Lafond C, Petit A, Lam Cham Kee D, Durdux C, Haie-Méder C. Radiotherapy of cervical cancer. *Cancer Radiother*. 2022 Feb-Apr;26(1–2):298–308.
3. Ucker DS, Levine JS. Exploitation of apoptotic regulation in Cancer. *Front Immunol*. 2018;9:241.
4. Huang Q, Li F, Liu X, Li W, Shi W, Liu FF, O'Sullivan B, He Z, Peng Y, Tan AC, Zhou L, Shen J, Han G, Wang XJ, Thorburn J, Thorburn A, Jimeno A, Raben D, Bedford JS, Li CY. Caspase 3-mediated stimulation of tumor cell repopulation during cancer radiotherapy. *Nat Med*. 2011;17(7):860–6.
5. Obenauf AC, Zou Y, Ji AL, Vanharanta S, Shu W, Shi H, Kong X, Bosenberg MC, Wiesner T, Rosen N, Lo RS, Massagué J. Therapy-induced tumour secretomes promote resistance and tumour progression. *Nature*. 2015;520(7547):368–72.
6. Pavlyukov MS, Yu H, Bastola S, Minata M, Shender VO, Lee Y, Zhang S, Wang J, Komarova S, Wang J, Yamaguchi S, Alsheikh HA, Shi J, Chen D, Mohyeldin A, Kim SH, Shin YJ, Anufrieva K, Evtushenko EG, Antipova NV, Arapidi GP, Govorun V, Pestov NB, Shakhparonov MI, Lee LJ, Nam DH, Nakano I. Apoptotic Cell-Derived extracellular vesicles promote malignancy of glioblastoma via intercellular transfer of splicing factors. *Cancer Cell*. 2018;34(1):119–e13510.
7. Li M, Liao L, Tian W. Extracellular vesicles derived from apoptotic cells: an essential link between death and regeneration. *Front Cell Dev Biol*. 2020;8:573511.
8. Han L, Xu J, Xu Q, Zhang B, Lam EW, Sun Y. Extracellular vesicles in the tumor microenvironment: therapeutic resistance, clinical biomarkers, and targeting strategies. *Med Res Rev*. 2017;37(6):1318–49.
9. Wang RA. MTA1—a stress response protein: a master regulator of gene expression and cancer cell behavior. *Cancer Metastasis Rev*. 2014;33(4):1001–9.
10. Hannafon BN, Gin AL, Xu YF, Bruns M, Calloway CL, Ding WQ. Metastasis-associated protein 1 (MTA1) is transferred by exosomes and contributes to the regulation of hypoxia and Estrogen signaling in breast cancer cells. *Cell Commun Signal*. 2019;17(1):13.
11. Min HY, Lee HY. Cellular dormancy in cancer: mechanisms and potential targeting strategies. *Cancer Res Treat*. 2023;55(3):720–36.
12. Tamamouna V, Pavlou E, Neophytou CM, Papageorgis P, Costeas P. Regulation of metastatic tumor dormancy and emerging opportunities for therapeutic intervention. *Int J Mol Sci*. 2022;23(22):13931.
13. Bragado P, Sosa MS, Keely P, Condeelis J, Aguirre-Ghiso JA. Microenvironments dictating tumor cell dormancy. *Recent Results Cancer Res*. 2012;195:25–39.
14. Kurppa KJ, Liu Y, To C, Zhang T, Fan M, Vajdi A, Knelson EH, Xie Y, Lim K, Cejas P, Portell A, Lizotte PH, Ficarro SB, Li S, Chen T, Haikala HM, Wang H, Bahcall M, Gao Y, Shalhout S, Boettcher S, Shin BH, Thai T, Wilkens MK, Tillgren ML, Mushajiang M, Xu M, Choi J, Bertram AA, Ebert BL, Beroukhir R, Bandopadhyay P, Awad MM, Gokhale PC, Kirschmeier PT, Marto JA, Camargo FD, Haq R, Paweletz CP, Wong KK, Barbie DA, Long HW, Gray NS, Jänne PA. Treatment-Induced tumor dormancy through YAP-Mediated transcriptional reprogramming of the apoptotic pathway. *Cancer Cell*. 2020;37(1):104–e12212.
15. Muller L, Hong CS, Stolz DB, Watkins SC, Whiteside TL. Isolation of biologically active exosomes from human plasma. *J Immunol Methods*. 2014;411:55–65.
16. Katakowski M, Buller B, Zheng X, Lu Y, Rogers T, Osobamiro O, Shu W, Jiang F, Chopp M. Exosomes from marrow stromal cells expressing miR-146b inhibit glioma growth. *Cancer Lett*. 2013;335(1):201–4.
17. Franken NA, Rodermond HM, Stap J, Haveman J, van Bree C. Clonogenic assay of cells in vitro. *Nat Protoc*. 2006;1(5):2315–9.
18. Deng YR, Chen XJ, Chen W, Wu LF, Jiang HP, Lin D, Wang LJ, Wang W, Guo SQ. Sp1 contributes to radioresistance of cervical cancer through targeting G2/M cell cycle checkpoint CDK1. *Cancer Manag Res*. 2019;11:5835–44.
19. Choudhary GS, Al-Harbi S, Almasan A. Caspase-3 activation is a critical determinant of genotoxic stress-induced apoptosis. *Methods Mol Biol*. 2015;1219:1–9.
20. Zhou J, Lei N, Tian W, Guo R, Chen M, Qiu L, Wu F, Li Y, Chang L. Recent progress of the tumor microenvironmental metabolism in cervical cancer radioresistance. *Front Oncol*. 2022;12:999643.
21. Wong RS. Apoptosis in cancer: from pathogenesis to treatment. *J Exp Clin Cancer Res*. 2011;30(1):87.
22. Plesca D, Mazumder S, Almasan A. DNA damage response and apoptosis. *Methods Enzymol*. 2008;446:107–22.
23. Fan TJ, Han LH, Cong RS, Liang J. Caspase family proteases and apoptosis. *Acta Biochim Biophys Sin (Shanghai)*. 2005;37(11):719–27.
24. Sunderland A, Williams J, Andreou T, Rippaus N, Fife C, James F, Kartika YD, Speirs V, Carr I, Droop A, Lorgier M. Biglycan and reduced Glycolysis are associated with breast cancer cell dormancy in the brain. *Front Oncol*. 2023;13:1191980.
25. Davis JE Jr, Kirk J, Ji Y, Tang DG. Tumor dormancy and Slow-Cycling Cancer cells. *Adv Exp Med Biol*. 2019;1164:199–206.
26. Aguirre-Ghiso JA, Estrada Y, Liu D, Ossowski L. ERK(MAPK) activity as a determinant of tumor growth and dormancy; regulation by p38(SAPK). *Cancer Res*. 2003;63(7):1684–95.
27. Morana O, Wood W, Gregory CD. The apoptosis paradox in Cancer. *Int J Mol Sci*. 2022;23(3):1328.
28. Caruso S, Poon IKH. Apoptotic Cell-Derived extracellular vesicles: more than just debris. *Front Immunol*. 2018;9:1486.
29. Kakarla R, Hur J, Kim YJ, Kim J, Chwae YJ. Apoptotic cell-derived exosomes: messages from dying cells. *Exp Mol Med*. 2020;52(1):1–6.
30. He S, Cheng J, Sun L, Wang Y, Wang C, Liu X, Zhang Z, Zhao M, Luo Y, Tian L, Li C, Huang Q. HMGB1 released by irradiated tumor cells promotes living tumor cell proliferation via paracrine effect. *Cell Death Dis*. 2018;9(6):648.
31. Feng X, Yu Y, He S, Cheng J, Gong Y, Zhang Z, Yang X, Xu B, Liu X, Li CY, Tian L, Huang Q. Dying glioma cells Establish a proangiogenic microenvironment through a caspase 3 dependent mechanism. *Cancer Lett*. 2017;385:12–20.
32. Maacha S, Bhat AA, Jimenez L, Raza A, Haris M, Uddin S, Grivel JC. Extracellular vesicles-mediated intercellular communication: roles in the tumor microenvironment and anti-cancer drug resistance. *Mol Cancer*. 2019;18(1):55.
33. Gregory CD, Rimmer MP. Extracellular vesicles arising from apoptosis: forms, functions, and applications. *J Pathol*. 2023;260(5):592–608.
34. Gregory CD, Paterson M. An apoptosis-driven 'onco-regenerative niche': roles of tumour-associated macrophages and extracellular vesicles. *Philos Trans R Soc Lond B Biol Sci*. 2018;373(1737):20170003.
35. Gregory CD, Dransfield I. Apoptotic tumor Cell-Derived extracellular vesicles as important regulators of the Onco-Regenerative niche. *Front Immunol*. 2018;9:1111.
36. Horrevorts SK, Stolk DA, van de Ven R, Hulst M, van Het Hof B, Duinkerken S, Heineke MH, Ma W, Dusoswa SA, Nieuwland R, Garcia-Vallejo JJ, van de Loosdrecht AA, de Grujijl TD, van Vliet SJ, van Kooyk Y. Glycan-Modified apoptotic

- Melanoma-Derived extracellular vesicles as antigen source for Anti-Tumor vaccination. *Cancers (Basel)*. 2019;11(9):1266.
37. Sen N, Gui B, Kumar R. Role of MTA1 in cancer progression and metastasis. *Cancer Metastasis Rev*. 2014;33(4):879–89.
 38. Moon HE, Cheon H, Chun KH, Lee SK, Kim YS, Jung BK, Park JA, Kim SH, Jeong JW, Lee MS. Metastasis-associated protein 1 enhances angiogenesis by stabilization of HIF-1 α . *Oncol Rep*. 2006;16(4):929–35.
 39. Wang T, Sun F, Li C, Nan P, Song Y, Wan X, Mo H, Wang J, Zhou Y, Guo Y, Helali AE, Xu D, Zhan Q, Ma F, Qian H. MTA1, a novel ATP synthase complex modulator, enhances Colon cancer liver metastasis by driving mitochondrial metabolism reprogramming. *Adv Sci (Weinh)*. 2023;10(25):e2300756.
 40. Li DQ, Yang Y, Kumar R. MTA family of proteins in DNA damage response: mechanistic insights and potential applications. *Cancer Metastasis Rev*. 2014;33(4):993–1000.
 41. Xin B, Wang XY, Li Y, Qin JH, Ma XJ, Yin JP, Wang RA. [Expression and potential role of metastasis-associated protein 1 in the induced carcinogenesis of mouse liver]. *Xi Bao Yu Fen Zi Mian Yi Xue Za Zhi*. 2012;28(8):801–3. Chinese.
 42. Gomatou G, Syrigos N, Vathiotis IA, Kotteas EA. Tumor dormancy: implications for invasion and metastasis. *Int J Mol Sci*. 2021;22(9):4862.
 43. Chen J, Li Y, Yu TS, McKay RM, Burns DK, Kernie SG, Parada LF. A restricted cell population propagates glioblastoma growth after chemotherapy. *Nature*. 2012;488(7412):522–6.
 44. Sosa MS, Parikh F, Maia AG, Estrada Y, Bosch A, Bragado P, Ekin E, George A, Zheng Y, Lam HM, Morrissey C, Chung CY, Farias EF, Bernstein E, Aguirre-Ghiso JA. NR2F1 controls tumour cell dormancy via SOX9- and RAR β -driven quiescence programmes. *Nat Commun*. 2015;6:6170.
 45. Wu R, Roy AM, Tokumaru Y, Gandhi S, Asaoka M, Oshi M, Yan L, Ishikawa T, Takabe K. NR2F1, a tumor dormancy marker, is expressed predominantly in Cancer-Associated fibroblasts and is associated with suppressed breast Cancer cell proliferation. *Cancers (Basel)*. 2022;14(12):2962.
 46. Recasens A, Munoz L. Targeting Cancer cell dormancy. *Trends Pharmacol Sci*. 2019;40(2):128–41.
 47. Borgen E, Rypdal MC, Sosa MS, Renolen A, Schlichting E, Lønning PE, Synnestvedt M, Aguirre-Ghiso JA, Naume B. NR2F1 stratifies dormant disseminated tumor cells in breast cancer patients. *Breast Cancer Res*. 2018;20(1):120.
 48. Cackowski FC, Eber MR, Rhee J, Decker AM, Yumoto K, Berry JE, Lee E, Shiozawa Y, Jung Y, Aguirre-Ghiso JA, Taichman RS. Mer tyrosine kinase regulates disseminated prostate Cancer cellular dormancy. *J Cell Biochem*. 2017;118(4):891–902.
 49. Sosa MS, Bragado P, Aguirre-Ghiso JA. Mechanisms of disseminated cancer cell dormancy: an awakening field. *Nat Rev Cancer*. 2014;14:611–22.
 50. Phan TG, Croucher PI. The dormant cancer cell life cycle. *Nat Rev Cancer*. 2020;20(7):398–411.
 51. Prunier C, Baker D, Ten Dijke P, Ritsma L. TGF- β family signaling pathways in cellular dormancy. *Trends Cancer*. 2019;5(1):66–78.
 52. Adam AP, George A, Schewe D, Bragado P, Iglesias BV, Ranganathan AC, Kourtidis A, Conklin DS, Aguirre-Ghiso JA. Computational identification of a p38SAPK-regulated transcription factor network required for tumor cell quiescence. *Cancer Res*. 2009;69(14):5664–72.
 53. Bragado P, Estrada Y, Parikh F, Krause S, Capobianco C, Farina HG, Schewe DM, Aguirre-Ghiso JA. TGF- β 2 dictates disseminated tumour cell fate in target organs through TGF- β -RIII and p38 α / β signalling. *Nat Cell Biol*. 2013;15(11):1351–61.
 54. Di Martino JS, Nobre AR, Mondal C, Taha I, Farias EF, Fertig EJ, Naba A, Aguirre-Ghiso JA, Bravo-Cordero JJ. A tumor-derived type III collagen-rich ECM niche regulates tumor cell dormancy. *Nat Cancer*. 2022;3(1):90–107.
 55. Yao YL, Yang WM. The metastasis-associated proteins 1 and 2 form distinct protein complexes with histone deacetylase activity. *J Biol Chem*. 2003;278(43):42560–8.
 56. Millard CJ, Watson PJ, Celardo I, Gordiyenko Y, Cowley SM, Robinson CV, Fairall L, Schwabe JW. Class I HDACs share a common mechanism of regulation by inositol phosphates. *Mol Cell*. 2013;51(1):57–67.
 57. Markou A, Tzanikou E, Lianidou E. The potential of liquid biopsy in the management of cancer patients. *Semin Cancer Biol*. 2022;34:69–79.
 58. Lihon MV, Hadisurya M, Wu X, Iliuk A, Tao WA. Isolation and identification of plasma extracellular vesicles protein biomarkers. *Methods Mol Biol*. 2023;2660:207–17.

Publisher's note

Springer Nature remains neutral with regard to jurisdictional claims in published maps and institutional affiliations.